The Increase in Sagittal Sinus Size in Multiple Sclerosis: Elevated Venous Pressure or Increased Wall Stiffness, a Feasibility Study

Grant Alexander Bateman (grant.bateman@health.nsw.gov.au)
John Hunter Hospital
Jeannette Lechner-Scott
Hunter Medical Research Institute
Alexander Bateman
University of NSW

Article

Keywords: Multiple Sclerosis, elastic modulus, pressure gradient, modelling

Posted Date: April 13th, 2022

DOI: https://doi.org/10.21203/rs.3.rs-1543872/v1

Abstract

The cross-sectional area of the superior sagittal sinus (SSS) is larger in multiple sclerosis than normal and correlates with disease severity and progression. The sinus could be enlarged due to a decrease in the pressure difference between the lumen and the subarachnoid space, an increase in wall thickness or increased wall stiffness. The cross-sectional area of the SSS and straight sinus (ST) were measured in 103 patients with multiple sclerosis and compared to 50 controls. The cross-sectional area of the SSS and ST were increased by 20% and 13% compared to the controls ($p = 0.005$ and 0.02 respectively). The deflection of the wall of the sinus was estimated. The change in pressure gradient, wall thickness or elastic modulus between groups was calculated by modelling the walls as simply supported beams. To account for these findings, the modelling suggests either a 70% reduction in transmural venous pressure or a 3 fold increase in SSS wall stiffness plus an 11% increase in wall thickness. An increase in sinus pressure, although the most straight forward possibility to account for the change in sinus size, may be the least feasible. An increase in sinus wall stiffness and thickness may need further investigation.

Introduction

In multiple sclerosis (MS) the superior sagittal sinus (SSS) cross-sectional area was found to be 16% larger than in matched controls [1]. The sinus size seems to have prognostic significance with larger sinuses correlating with male patients, progressive forms of the disease and worsening outcomes [2]. It was noted that in hydrocephalus and spontaneous intracranial hypotension, the cross-sectional area of the SSS varies with the pressure difference between the sinus and the subarachnoid space (the transmural pressure) [1]. This suggests that the larger sinus size in MS could be due to a decrease in the transmural pressure. However, this interpretation is problematic because it was noted that a significant reduction in the transmural pressure would affect the CSF absorption across the sinus wall via the arachnoid granulations and cerebrospinal fluid (CSF) would need to be absorbed via an accessory route [3]. It was suggested that an alternative cause of the enlarged sinuses could be an increase in the stiffness of the sinus wall [1] but which of these alternatives is the more feasible?

The sagittal sinus consists of a venous channel passing through a split in the dura as it passes from the falx cerebri to the skull [4]. The dura at the base of the sinus is attached to the endosteum of the skull and is fixed. The other two walls of the sinus are attached to the falx cerebri and are relatively fixed at this point [1]. Between the three fixed vertices, the two free walls can move. In the transverse sinuses the free walls have been noted to be concave, straight or convex [5]. As previously noted, the walls of the sagittal sinus have also been shown to move depending on the transmural pressure gradient [1]. The dural wall is a viscoelastic structure made up of collagen fibers interspersed with fibroblasts and elastin [6], so the structural properties of the wall are also important in the degree of deflection. In engineering terms, the degree of sinus wall deflection is similar to the deflection seen in a beam under load (see Fig. 1). Deflection occurs in a beam which is freely supported at both ends due to a force which is equally applied along its length. The size of the deflection depends on the length of the beam, size of the force, the elastic modulus or stiffness and the beam thickness [7]. The elastic modulus can be estimated if the wall length,

deflection, wall thickness and the applied force are known [7]. Thus, the purpose of this paper is to use engineering modelling to test the feasibility of whether the sinus walls are altered in their deflection in MS due to an alteration in pressure, wall stiffness or wall thickness.

Results

The sinus length and cross-sectional area data is summarized in Table 1. The raw data is available online[8].

Table 1
SAGITTAL AND STRAIGHT SINUS MEASUREMENTS

		Control					
	Age years	SSS Area mm2	SSS length mm	SSS height mm	SSS triangle area mm	SSS chord length mm	ST area mm2
mean	44.9	45.0	12.6	7.9	51.6	10.2	15.7
SD	10.9	16.0	3.1	2.0	22.2	2.2	5.4
n	50						
		Multiple Sclerosis					
mean	47.8	54.0	13.5	8.1	56.4	10.6	17.8
SD	13.0	17.6	2.8	1.7	20.7	1.9	5.7
n	103						
MWU	0.28	0.005*	0.08	0.56	0.16	0.23	0.02*

Note.- mm, millimeters; mm2, millimeters squared; MWU, Mann-Whitney U test; SD, standard deviation; SSS, superior sagittal sinus; ST, straight sinus; *, significance < 0.05

The multiple sclerosis patient's SSS and straight sinus (ST) areas were 20% and 13% larger than the controls ($p = 0.005$ and 0.02 respectively). The sagittal sinus widths and the heights of the attachments from the baseline and vertex for the controls and MS patients were not significantly different. Therefore, the free wall lengths and the areas of the triangles subtended by the attachment points were not significantly different.

Modelling

The chord length from Table 1 for the controls is 10.2 mm and by subtraction the area of the deflection is the SSS area minus the SSS triangle area divided by 2 or 3.3 mm^2 per side. Using Eq. (1) this equates to a deflection of 0.48 mm. The normal ICP obtained from the literature is 11.5 mmHg [9]. The normal SSS

pressure is 7.5 mmHg at 45 years of age [10]. This gives a normal SSS transmural pressure by subtraction of 4 mmHg, which correlates the literature [11]. Modelling a strip of sinus wall 1mm wide (this width was chosen for simplicity but has no bearing on the final outcome) would give an area of the upper surface of 1mm x the chord length. Placing the area and pressure in Eq. (2) gives an equally applied force of 0.0054 Newtons. The median thickness of the free walls of the posterior portion of the SSS in a human cadaver study was 0.675 mm [12]. If we model a strip of dura 1mm wide, the moment of inertia of cross-section from Eq. (4) would be $2.56x10^{-14}$ m^4. Placing these values in Eq. (4) and solving for the elastic modulus gives a result of 6.1 MPa for the controls.

Using the same technique, the deflection in MS is 65% less than in the controls at 0.17 mm. Assuming the elastic modulus and wall thickness are unchanged from the controls, this would give a transmural pressure of 1.2 mmHg or a reduction in pressure of 70% compared to the controls. If we assume that transmural pressure and wall thickness are unchanged, then the elastic modulus would be increased to 20.1 MPa or 3.3 times normal. If the transmural pressure and elastic modulus were unchanged, then the wall thickness would be 1.0 mm or 1.49 times normal.

Discussion

The correct engineering model to use in the current study would depend on the type of boundary condition at the attachment points i.e. fixed, roller or pinned [7]. The use of a fixed condition would assume that the angle at the endpoint is zero with respect to the horizontal [7] (i.e. the attachment does not bend). As the angle at the attachment endpoints are non-zero, the most suitable model would require the equivalent of pinned endpoints i.e. the simply supported beam. The use of a roller condition would yield the same result as the pinned condition in this instance, as the same mathematical assumptions with regard to the beam deflection are used [7].

The modelling requires an estimate of the force applied across the sinus walls in the controls. Thus, we need to know the CSF and venous pressures. The normal ICP and sinus pressure and transmural pressures were obtained from the literature.

The modelling also requires an accurate estimate of the deflection of the walls. It became obvious that direct measurement of the deflection was too inaccurate. The resolution of the post contrast 3D T1 images is 0.85 mm with each pixel being 0.72 mm^2. The average deflection in the controls was 0.48 mm (half a pixel) but the combined reduction in the sinus area was 6.6 mm^2 and this represented approximately 9 pixels. Given the attachment points are relatively fixed, the deflection could be estimated from the change in the cross-sectional area. In a cadaver study of adults mean age 39 years, the sagittal sinus just above the Torcular was found to be an isosceles triangle of mean width 11.6 mm and height 8.3 mm with a 48 mm^2 cross-sectional area and a calculated average free wall length of 10.1 mm. [13]. These measurements are very similar to the mean width, height, triangle area and free wall length found in the present study, with the difference between the cadavers and control patients being 8%, 5%, 7% and 1% respectively. Sensitivity analysis suggests an 8% error in either the area or length measurement would

have a minimal effect on the final outcome of this study. There is no transmural pressure gradient in a cadaver, meaning the stress free state for the normal sinus walls is for them to be straight. Thus, they were compared to the calculated triangle sinus area. The length measurements in MS were not significantly different to the controls, indicating multiple sclerosis is unlikely to alter the fixed point positions. As a pressure gradient is equivalent to a force which is equally applied in all directions, the expected deflection when compared to the original straight wall position should approximate a circle segment. According to Laplace's law, when a pressure is applied to a thin membrane, the volume change will be accommodated by the smallest possible change in membrane area because this would give the minimum energy state. The smallest surface area for a given volume is always a circle segment. The same mechanism underlies why cerebral aneurysms develop as circle segments [14]. The deflection as seen in Fig. 2 was calculated from the area between the free wall or chord and the curved line using the circle Eq. (1).

In the controls, a small smooth deflection averaging 0.48 mm develops from a 4 mmHg pressure gradient, giving a Young's modulus averaging 6.1 MPa. The dural elastic modulus has been measured in humans using fresh samples with the values varying from 29.4 MPa [15], 44 MPa [16], up to 61 MPa [17]. The dura from these studies comes from various regions of the skull but to our knowledge the wall of the sinus has never been sampled in humans and it is possible that the differing regions may be optimised for varying degrees of absolute strength rather than flexibility. In pigs, the dura over the inner table of the skull has been measured to be between 8 and 16 MPa [18] i.e. the stiffness is somewhat less than that in humans. In pigs, the longitudinal and circumferential SSS stiffness within the occipital region has been measured and found to be 58.1 ± 17.2 MPa longitudinally with the circumferential figure being 3.0 ± 0.7 MPa [18]. The circumferential stiffness in pigs compares to the circumferential stiffness of 6.1 MPa we estimated, again suggesting human dura is somewhat stiffer than porcine. The difference between the longitudinal and circumferential stiffness in the SSS is due to the collagen alignment. The fraction of collagen within the pig sinus wall is 84%. The collagen is randomly directed in that portion of the sinus adjacent to the bone but is longitudinally directed in those portions adjacent to the subarachnoid space [18]. This suggests the free walls of the sinus are designed to be stiff in the longitudinal direction but flexible at 90 degrees to this direction.

The simplest explanation for the 20% larger sinus area in MS is an increase in sinus pressure compared to the subarachnoid pressure i.e. the transmural pressure. As discussed in the introduction, a decrease in the sagittal sinus transmural pressure would require an alternate route for CSF to be absorbed other than through the arachnoid granulations. The capillary bed drained by the deep venous system could possibility account for the CSF drainage but as noted, the straight sinus is increased in size in MS by 13% suggesting that both the superficial and deep drainage systems are similarly affected. In favour of the elevated pressure hypothesis, the transverse sinuses in MS patients have been found to have an average 39% effective stenosis in area and there was a 62% increase in jugular bulb height [2], with both of these findings suggested to increase venous pressure. However, this pressure increase is probably modest at best. Mathematical modelling of a 7.5 mm diameter cerebral vessel suggests a pressure drop across a stenosis of 40–50% by area would be only 1–2 mmHg [19]. A 38% area stenosis (almost identical to the

MS stenosis) in the sagittal sinus was estimated to increase the venous pressure by only 0.7 mmHg [20]. Given the jugular bulb pressure between MS and controls was noted to be unchanged [21], the sagittal sinus pressure may be possibly increased by 1–2 mmHg at most in MS but not the 2.8 mmHg increase as required by the modelling. However, even a 1–2 mmHg increase would be unlikely to affect the transmural pressure because although the normal ICP is 11.5 mmHg [9], the ICP measured at lumbar puncture in 32 MS patients was 12.9 ± 3.3 mmHg (1.4 mmHg higher), with the MS ICP being identical to normal pressure hydrocephalus patients [22]. Normal pressure hydrocephalus patients are known to have mildly elevated ICP which is still within normal range [23]. Thus, any mild increase in venous pressure in MS would only match the mild increase in ICP, giving a normal transmural pressure overall. Thus, the venous pressure theory causing sinus size change is probably not feasible.

The other possibility is a change in the structure of the sinus wall. The modelling suggests either a 3.3 times increase in wall stiffness or a 49% increase in wall thickness or perhaps a combination of both. By solving Eq. (3) for both the elasticity and wall thickness (using a normal pressure) in both the MS patients and controls and calculating the combined change in these two variables by division, it can be shown that the change in elasticity multiplied by the change in wall thickness cubed is equal to 3.3. Indicating which combinations of each variable would be possible.

$$\Delta E \times \Delta D^3 = 3.3 \quad (5)$$

In order to clarify the possibilities further we require an independent measurement. In MS the time taken for the arterial pulsation to pass into the SSS was reduced by 35% compared to controls [24]. This represents a measurement of the pulse wave velocity between the arteries and the venous system via the subarachnoid space including the spinal canal. The square of the pulse wave velocity within a vessel is equal to the elastic modulus multiplied by the wall thickness divided by two times the fluid density multiplied by the radius [25] i.e.

$$PWV^2 = E \times D / \rho \times R \quad (6)$$

The blood density is a constant and the difference in the sagittal sinus hydraulic diameter (proportional to the radius) in this cohort has been previously measured [2], which would allow the radial difference to be estimated. If the dura mater of the entire system (spinal canal and sinus walls) were similarly affected, then we can solve Eq. (6) for both the controls and MS patients and by division show that.

$$\Delta E \times \Delta D = 2.7 \quad (7)$$

The mechanical response of the spinal canal and sinus walls have been shown to be similarly affected by MS with spinal canal pulsation propagation reduced by 40% and the venous sinus propagation by 50% [24]. Solving Eqs. (5) and (7) simultaneously gives a change in wall stiffness of 3 times normal and wall thickness of 1.11 times normal. Is a 3 fold increase in circumferential wall stiffness feasible? As previously discussed, the longitudinal stiffness is much higher (approximately 20 fold) than the circumferential stiffness in the SSS due to the longitudinal orientation of the fibers. Reorientation of the

fibers into a random distribution could increase the circumferential stiffness by enough to make the findings feasible. There is chronic inflammation of the vein walls in MS. Forty seven percent of MS patients showed evidence of dural inflammation, which was equally distributed across all age groups i.e. it is likely chronic [26]. Chronic inflammation could cause the fibers to be reoriented secondary to remodeling and scarring. There is a change in type 1 collagen in the jugular veins in MS with microcalcification deposition [27], similarly suggesting structural wall changes. Finally, there is a 10 fold increased risk of MS in Ehlers-Danlos syndrome (EDS) patients [28]. EDS is characterized by altered collagen synthesis and enzyme dysfunction [29]. EDS is usually thought to be associated with decreased vascular stiffness, however, one paper has suggested an increased arterial stiffness occurs compared to controls [30]. Cell culture of fibroblasts indicates that there is a significant reduction in directional fiber orientation in EDS compared to normal [31], suggesting a random distribution of fibers in the SSS could increase circumferential stiffness but decrease the longitudinal stiffness.

Methods

Subjects

One hundred and three MS patients were prospectively recruited from an MS outpatient clinic at a tertiary referral hospital. These patients were part of a previous study [2]. There were 79 females and 24 males of average age 47.8 ± 13.0 years. There were 90 patients with relapsing remitting MS, 11 with secondary progressive MS and 2 with primary progressive MS. The clinical information regarding these patients can be found in the online data set [32]. The patients were matched to 50 previously published control patients undergoing pre-op MRI studies for stereotactic surgery for lesions thought to be unlikely to alter the intracranial pressure or compliance [3]. The surgery was for indications such as pituitary microadenoma, trigeminal artery decompression or a small meningioma less than 2 cm in size. There were 37 females and 13 males of average age 44.9 ± 10.9 years.

Ethics approval and informed consent

Informed consent

was obtained from all patients enrolled in this study. The study was approved by the Hunter New England Area Health Ethics Committee, therefore, the study has been performed in accordance with the ethical standards laid down in the 1964 Declaration of Helsinki. The authorization number 2019ETH00912 was issued.

MR and Analysis

The patients were imaged on a 1.5 T superconducting magnet (Magnetom Avanto; Seimens, Erlangen Germany). In all MS patients, a standard brain MRI consisting of 3DT1and 3DFLAIR sagittal, T2 axial and diffusion weighted axial images was performed followed by 3DT1 post contrast imaging. All controls underwent the same pre and post contrast series, which had a 0.85 mm isotropic resolution. The MRI

imaging was sourced from the hospital picture archiving and communication system (PACS) and therefore all measurements were performed on the original data.

The 3DT1 post contrast data was reformatted using the MPR software on the scanner to display the cross-section of the sinuses. A slice perpendicular to the long axis of the sagittal sinus 3 cm above the Torcular was selected. The attachment points of the two free walls of the SSS with both the falx cerebri and the inner table of the skull were defined (see Fig. 1b and 2). The length of the base of the sinus was measured for each individual. The height was measured as a line taken perpendicular to the base line centered on the vertex at the falx. The length of the free walls were calculated using Pythagoras' theorem and designated the chord length. The triangular area of the sinus was calculated as half the base length times the height. Finally, the actual sinus area was measured by manually drawing around the sinus using the scanners measurement tool. Any sinus area below the baseline was ignored. The area of the straight sinus was measured similar to the SSS area.

The deflection of the sinus wall was estimated from the change in cross-sectional area between the actual sinus measurement and the sinus triangle area (see Fig. 2) and the chord length, using the formula for the segment of a circle:

$A \approx 2/3\ s*h + h^3/2s$ (1)

The error in this approximation is 0.1% for 0° $\theta \leq 150°$ where θ is the angle subtended by the chord at the circle centre. A is the area between the chord and circle segment. Variable "s" is the chord length (a chord is a line which intersects a circle to produce a segment) and h is the chord height measured from the centre of the chord to the circle segment [33]. The chord height is equivalent to the sinus wall deflection. The equally distributed force can be found from the transmural pressure using the formula:

$F = P \times A$ (2)

P is the applied transvenous pressure and A is the cross-sectional area of the upper surface of the chord [34].

The formula for a simply supported beam relates the deflection of a beam to its mechanical properties. For a simply supported beam the following equation governs the maximum deflection produced by an equally distributed force:

$D= (5 \times F \times L^3)/ (384 \times E \times I)$ (3)

D is the maximum deflection which is located at the centre of the beam, F is the force, L is the length of the beam, E is the modulus of elasticity and I is the moment of inertia of cross-section [34].

The moment of inertia of cross-section is a constant related to the geometry of the beam:

$I= (W \times D^3)/ 12$ (4)

W is the beam width and D is the height of the beam. All variables are in S.I. units.

Statistical analysis

Mean and standard deviations were obtained for each group. A Shapiro-Wilk Test was used to test for normality of the data. Differences between the groups were tested using a Mann-Whitney U test. An $\alpha \leq 0.05$ was used to assess statistical significance for all tests.

Declarations

Author's contributions

Conceptualisation and design GAB, ARB. Imaging data acquisition GAB. Clinical data acquisition JLS. Mathematical analysis and statistics ARB. Data curation GAB, JLS. Writing- original draft GAB; Writing-review& editing all authors.

Competing interests

The authors declare that they have no competing interests.

Availability of data

All data generated or analysed during this study are included in this published article. The raw data is available online.

Funding

This research did not receive any specific grant from funding agencies in the public, commercial, or not-for-profit sectors.

Not applicable

References

1. Bateman, G. A., Lechner-Scott, J., Copping, R., Moeskops, C. & Yap, S. L. Comparison of the sagittal sinus cross-sectional area between patients with multiple sclerosis, hydrocephalus, intracranial hypertension and spontaneous intracranial hypotension: a surrogate marker of venous transmural pressure? Fluids Barriers CNS **14**, 18, doi:10.1186/s12987-017-0066-1 (2017).
2. Bateman, G. A., Lechner-Scott, J., Carey, M. F., Bateman, A. R. & Lea, R. A. Possible Markers of Venous Sinus Pressure Elevation in Multiple Sclerosis: Correlations with Gender and Disease Progression. Mult Scler Relat Disord **55**, 103207, doi:10.1016/j.msard.2021.103207 (2021).
3. Bateman, G. A., Lechner-Scott, J., Bateman, A. R., Attia, J. & Lea, R. A. The Incidence of Transverse Sinus Stenosis in Multiple Sclerosis: Further Evidence of Pulse Wave Encephalopathy. Mult Scler Relat Disord **46**, 102524, doi:10.1016/j.msard.2020.102524 (2020).

4. Sinnatamby, C. S. & Last, R. J. *Last's anatomy: regional and applied*. 12th edn, (Churchill Livingstone/Elsevier, 2011).
5. Farb, R. I., Forghani, R., Lee, S. K., Mikulis, D. J. & Agid, R. The venous distension sign: a diagnostic sign of intracranial hypotension at MR imaging of the brain. AJNR Am J Neuroradiol **28**, 1489–1493, doi:10.3174/ajnr.A0621 (2007).
6. Vandenabeele, F., Creemers, J. & Lambrichts, I. Ultrastructure of the human spinal arachnoid mater and dura mater. J Anat **189** (**Pt 2**), 417–430 (1996).
7. Hibbeler, R. C. *Mechanics of materials*. Ninth edition. edn, (Prentice Hall, 2014).
8. Bateman, G., Lechner-Scott, J. & Bateman, A. Multiple Sclerosis 2022. Mendeley Data **V2**, doi:10.17632/h943m59zmr.2 (2022).
9. Fleischman, D. *et al.* Cerebrospinal fluid pressure decreases with older age. PLoS One **7**, e52664, doi:10.1371/journal.pone.0052664 (2012).
10. Bateman, G. A. & Siddique, S. H. Cerebrospinal fluid absorption block at the vertex in chronic hydrocephalus: obstructed arachnoid granulations or elevated venous pressure? Fluids Barriers CNS **11**, 11, doi:10.1186/2045-8118-11-11 (2014).
11. Benabid, A. L., De Rougemont, J. & Barge, M. [Cerebral venous pressure, sinus pressure and intracranial pressure]. Neurochirurgie **20**, 623–632 (1974).
12. Balik, V. *et al.* Variability in Wall Thickness and Related Structures of Major Dural Sinuses in Posterior Cranial Fossa: A Microscopic Anatomical Study and Clinical Implications. Oper Neurosurg (Hagerstown) **17**, 88–96, doi:10.1093/ons/opy287 (2019).
13. Bruno-Mascarenhas, M. A., Ramesh, V. G., Venkatraman, S., Mahendran, J. V. & Sundaram, S. Microsurgical anatomy of the superior sagittal sinus and draining veins. Neurol India **65**, 794–800, doi:10.4103/neuroindia.NI_644_16 (2017).
14. Hademenos, G. J. The Physics of Cerebral Aneurysms. Physics Today **48**, 24–30, doi:10.1063/1.881442 (1995).
15. van Noort, R., Black, M. M., Martin, T. R. & Meanley, S. A study of the uniaxial mechanical properties of human dura mater preserved in glycerol. Biomaterials **2**, 41–45, doi:10.1016/0142-9612(81)90086-7 (1981).
16. Chauvet, D. *et al.* Histological and biomechanical study of dura mater applied to the technique of dura splitting decompression in Chiari type I malformation. Neurosurg Rev **33**, 287–294; discussion 295, doi:10.1007/s10143-010-0261-x (2010).
17. McGarvey, K. A., Lee, J. M. & Boughner, D. R. Mechanical suitability of glycerol-preserved human dura mater for construction of prosthetic cardiac valves. Biomaterials **5**, 109–117, doi:10.1016/0142-9612(84)90011-5 (1984).
18. Walsh, D. R., Lynch, J. J., DT, O. C., Newport, D. T. & Mulvihill, J. J. E. Mechanical and structural characterisation of the dural venous sinuses. Sci Rep **10**, 21763, doi:10.1038/s41598-020-78694-4 (2020).

19. Warwick, R., Sastry, P., Fontaine, E. & Poullis, M. Carotid artery diameter, plaque morphology, and hematocrit, in addition to percentage stenosis, predict reduced cerebral perfusion pressure during cardiopulmonary bypass: a mathematical model. J Extra Corpor Technol **41**, 92–96 (2009).
20. Bateman, G. A. & Bateman, A. R. Differences in the Calculated Transvenous Pressure Drop between Chronic Hydrocephalus and Idiopathic Intracranial Hypertension. AJNR Am J Neuroradiol **40**, 68–73, doi:10.3174/ajnr.A5883 (2019).
21. Zamboni, P. *et al.* Chronic cerebrospinal venous insufficiency in patients with multiple sclerosis. J Neurol Neurosurg Psychiatry **80**, 392–399, doi:10.1136/jnnp.2008.157164 (2009).
22. Ragauskas, A. *et al.* Improved diagnostic value of a TCD-based non-invasive ICP measurement method compared with the sonographic ONSD method for detecting elevated intracranial pressure. Neurol Res **36**, 607–614, doi:10.1179/1743132813Y.0000000308 (2014).
23. Silverberg, G. D. *et al.* Downregulation of cerebrospinal fluid production in patients with chronic hydrocephalus. J Neurosurg **97**, 1271–1275, doi:10.3171/jns.2002.97.6.1271 (2002).
24. Bateman, G. A., Lechner-Scott, J. & Lea, R. A. A comparison between the pathophysiology of multiple sclerosis and normal pressure hydrocephalus: is pulse wave encephalopathy a component of MS? Fluids Barriers CNS **13**, 18, doi:10.1186/s12987-016-0041-2 (2016).
25. Best, C. H., Taylor, N. B. & Brobeck, J. R. *Best & Taylor's Physiological basis of medical practice*. 10th edn, (Williams & Wilkins Co., 1979).
26. Hildesheim, F. E. *et al.* Leptomeningeal, dura mater and meningeal vessel wall enhancements in multiple sclerosis. Mult Scler Relat Disord **47**, 102653, doi:10.1016/j.msard.2020.102653 (2021).
27. Coen, M. *et al.* Altered collagen expression in jugular veins in multiple sclerosis. Cardiovasc Pathol **22**, 33–38, doi:10.1016/j.carpath.2012.05.005 (2013).
28. Vilisaar, J., Harikrishnan, S., Suri, M. & Constantinescu, C. S. Ehlers-Danlos syndrome and multiple sclerosis: a possible association. Mult Scler **14**, 567–570, doi:10.1177/1352458507083187 (2008).
29. Bergeron, M. E., Child, T. & Fatum, M. In vitro maturation and surrogacy in patients with vascular-type Ehlers-Danlos syndrome–a safe assisted reproductive technology approach. Hum Fertil (Camb) **17**, 141–144, doi:10.3109/14647273.2014.903002 (2014).
30. Roeder, M. *et al.* Increased augmentation index in patients with Ehlers-Danlos syndrome. BMC Cardiovasc Disord **20**, 417, doi:10.1186/s12872-020-01684-x (2020).
31. Micha, D., Pals, G., Smit, T. H. & Ghazanfari, S. An in vitro model to evaluate the properties of matrices produced by fibroblasts from osteogenesis imperfecta and Ehlers-Danlos Syndrome patients. Biochem Biophys Res Commun **521**, 310–317, doi:10.1016/j.bbrc.2019.09.081 (2020).
32. Bateman, G., Lechner-Scott, J., Carey, M., Bateman, A. & lea, R. Multiple sclerosis 2021. Mendeley Data, doi:10.17632/ndtxn2r2fg.1 (2021).
33. Harris, J. W. & Stocker, H. *Handbook of Mathematics and Computational Science*. 92–93 (Springer-Verlag, 1998).
34. Gere, J. M. & Goodno, B. J. *Mechanics of materials*. 8th edn, (Cengage Learning, 2013).

Figures

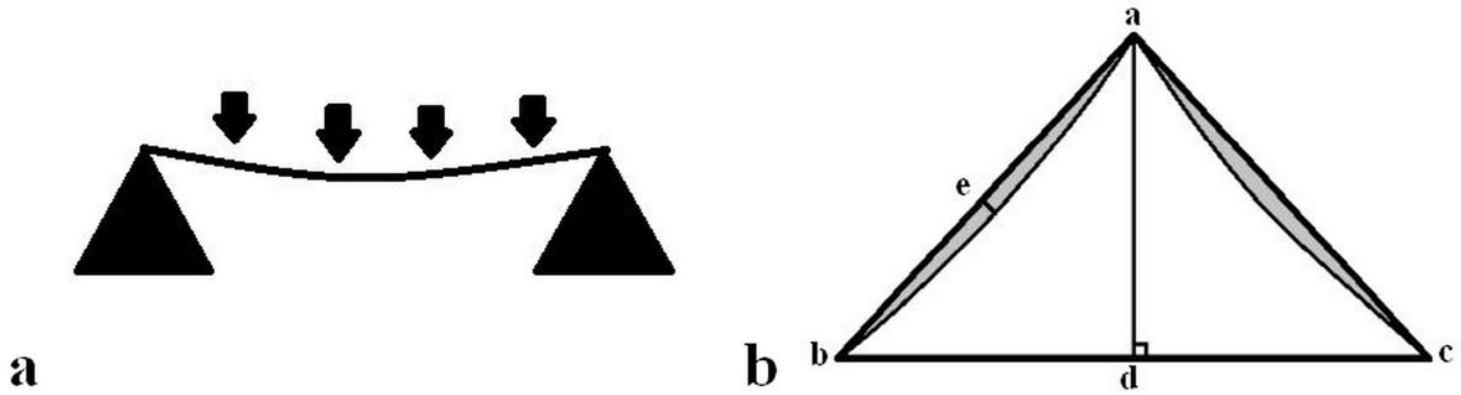

Figure 1

Free wall deflection as a simply supported beam

Fig. 1a A line drawing showing that a simply supported beam will deflect when under an equally distributed force depending on the size of the force, the beam length, thickness and stiffness,

Fig. 1b A line drawing of an idealized sagittal sinus. Point “a” is at the falx vertex and both “b” and “c” are the bony attachments. If the attachments are fixed in position is can be shown that the two free walls a-b and a-c would be deflected inwards by the transmural pressure similar to the simply supported beam. The difference in the area between the triangle subtended by the vertices and the actual area (shown in grey) is related to the deflection distance at “e” by the length a-b using equation (1). The perpendicular height is the line a-d.

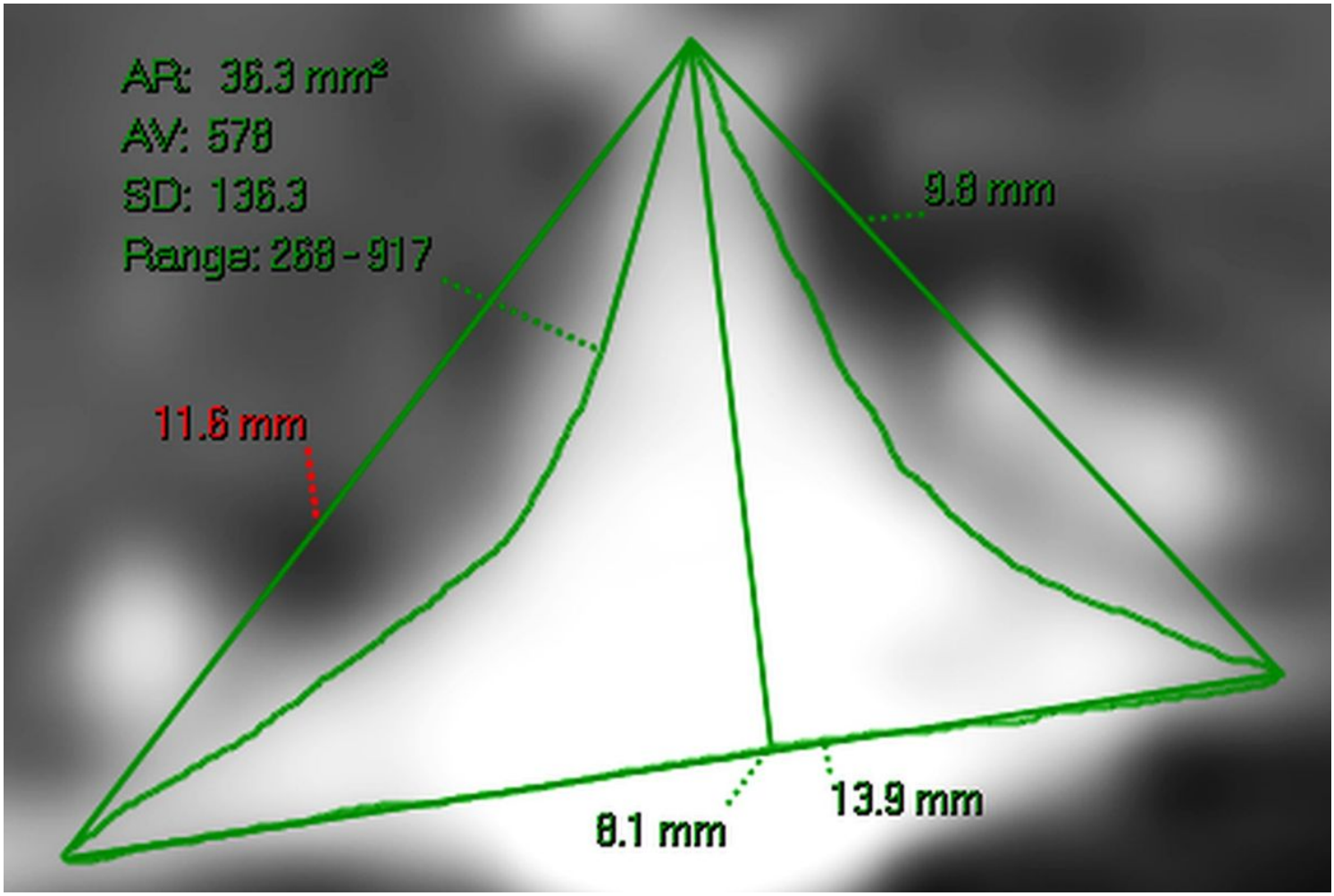

Figure 2

Measurements in a control patient

Fig. 2 A reconstruction of the 3DT1 post contrast data from a control patient. The baseline length is 13.9 mm and the perpendicular height is 8.1 mm giving a triangle area of 56.3 mm2. The deflection area on each side averages 10 mm2 (56.3-36.3/2). The average chord length between the vertex and both base attachments is 10.7 mm using Pythagoras' theorem. Giving an average deflection distance using equation (1) of 1.4 mm which is equivalent to the actual deflection in this case. Note, any sinus area below the baseline is ignored in this modelling study.